

Slowing and cooling molecules and neutral atoms by time-varying electric-field gradients

Jason A. Maddi,^{1,2,*} Timothy P. Dinneen,^{1,†} and Harvey Gould^{1,‡}

¹*Mail Stop 71-259, Lawrence Berkeley National Laboratory, University of California at Berkeley, Berkeley, California 94720*

²*Department of Physics, University of California at Berkeley, Berkeley, California 94720*

(Received 25 May 1999)

A method of slowing, accelerating, cooling, and bunching molecules and neutral atoms using time-varying electric-field gradients is demonstrated with cesium atoms in a fountain. The effects are measured and found to be in agreement with our calculations. Time-varying electric-field-gradient slowing and cooling is applicable to atoms that have large dipole polarizabilities, including atoms that are not amenable to laser slowing and cooling, to Rydberg atoms, and to molecules, especially polar molecules with large electric dipole moments. The possible applications of this method include slowing and cooling thermal beams of atoms and molecules, launching cold atoms from a trap into a fountain, and measuring atomic dipole polarizabilities.
[S1050-2947(99)01211-1]

PACS number(s): 32.60.+i, 32.80.Pj, 33.80.Ps, 33.55.Be

I. INTRODUCTION

Time-invariant electric-field gradients have long been used to deflect beams of molecules and neutral atoms. However, as we will show in this paper, time-varying electric-field gradients can be used to accelerate, slow, cool, or bunch these same beams. We demonstrate slowing, cooling, and bunching of cold cesium atoms in a fountain, measure these effects, and find good agreement with the calculation. The possible applications of the time-varying electric-field gradient technique include slowing and cooling thermal beams of molecules and atoms, launching cold atoms from a trap into a fountain, beam transport, and measuring atomic dipole polarizabilities.

The principle behind time-varying electric-field gradient slowing is that an electric-field gradient exerts a force on an electric dipole (thus accelerating or decelerating it) but a spatially uniform electric field, even if it is time varying, exerts no force on an electric dipole. Thus, an atom with an induced electric dipole moment or a molecule with a “permanent” electric dipole moment (with negative interaction energy in an electric field) will accelerate when it enters an electric field and decelerate back to its original velocity when it leaves the electric field. If we add a uniform electric field region between the entrance and exit, as in a pair of parallel electric field plates (Fig. 1), we can delay turning on the electric field until the atom or molecule is in this uniform electric field. The atom or molecule will not have accelerated entering the electric-field plates but will decelerate when it leaves the electric field, thus slowing. Longitudinal cooling is achieved by applying a decreasing electric field, so that in a pulse of atoms or molecules, the fastest ones, arriving first, experience the greatest slowing (Fig. 2).

The time-varying electric-field-gradient technique can be useful for slowing and cooling thermal beams of atoms with

large dipole polarizabilities and polar molecules with large electric dipole moments. Many atoms and most molecules are not amenable to laser slowing and cooling, and presently few alternative techniques [1] exist. Slow molecules have application to molecular-beam spectroscopy [2], the study of chemical reactions [3], low-energy collisions, surface scattering [4,5], and trapping [6–13].

The paper is organized as follows. The interaction energies of atoms and molecules in electric fields and the principles of slowing, cooling, and bunching molecules and atoms with time-varying electric-field gradients are discussed in detail in Sec. II. Our experiment is described and its results are compared with the calculation in Sec. III. And finally, in Sec. IV, we examine how the time-varying electric-field-gradient method can be applied to the slowing of thermal atoms and molecules, measurements of atomic dipole polarizabilities, atom optics, and launching atoms from traps.

II. ATOMS AND MOLECULES IN ELECTRIC FIELDS

A. Neutral atoms in electric fields

Time-varying electric-field-gradient slowing utilizes the shift in an atom’s potential energy as it travels through a time and spatially varying electric field. The effect of an electric field on an atom’s potential energy is described, to lowest order in the electric field, by the dipole polarizability of the atom, defined as the ratio of the induced electric dipole moment to the external electric field [14,15]. Although the dipole polarizability is a tensor, the nonscalar terms are usually small, producing only negligible variations in the polarizability of the different ground-state sublevels [14,15], and do not affect the processes that we will be discussing. Thus, the induced dipole moment is, to a good approximation, a scalar, and the potential energy \mathcal{E} is given to lowest order in the electric field by $\mathcal{E} = -\alpha E^2/2$, where E is the magnitude of the electric field and α is the scalar dipole polarizability. Because α is a scalar, the potential energy depends only on the electric field’s magnitude and not its direction.

In a spatially varying electric field, the force is $\mathbf{F} = (1/2)\alpha\nabla(E^2)$ that for all ground-state atoms is in the di-

*Electronic address: jamaddi@lbl.gov

†Present address: JILA, University of Colorado, Boulder CO 80309-0440.

‡Electronic address: gould@lbl.gov

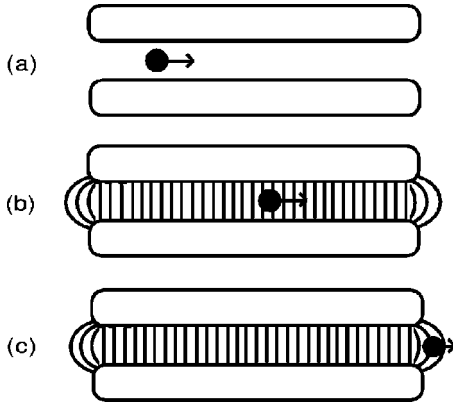


FIG. 1. Schematic diagram of slowing with a time-varying electric-field gradient. Molecules or neutral atoms enter the plates with the electric field turned off (a). When they are between the plates, a voltage is applied producing a spatially uniform electric field (b). They exit the plates, traversing an electric-field gradient where they are slowed (c). This process may be repeated with additional sets of electric-field plates.

rection of increasing electric-field magnitude (strong field seeking). As with any conservative potential, the change in an atom's kinetic energy as it travels between two points in space is path independent and equal to the change in potential energy between those points.

For example, a Cs atom traveling from a region E_i of no field to a region E_f of 10^7 V/m gains kinetic energy, E_{kin} , by an amount $\Delta E_{\text{kin}} = -\Delta\mathcal{E} = \alpha(E_f^2 - E_i^2)/2 = 3.3 \times 10^{-25}$ J = 24 mK, where we have used the value of 6.63×10^{-39} J/(V/m)² (or 59.6×10^{-24} cm³) for the dipole polarizability of Cs [16,17]. Since we will be interested in atomic beams from thermal sources (see Sec. IV), we will use energy units of kelvin with the conversion 7.243×10^{22} K/J. The velocity of an atom after traversing the potential is $v_f^2 = 2(\Delta E_{\text{kin}})/M + v_i^2$, where v_i and v_f are the initial and final velocities, respectively, and M is the mass. For $v_i=0$, the final velocity for the example given above would be 1.70 m/s.

B. Polar molecules in electric fields

In addition to a dipole polarizability, polar molecules have an intrinsic separation of charge that produces a dipole that can align with an external electric field to yield a large net electric dipole moment [18]. When the interaction of the electric dipole moment d_e of a linear polar molecule with an external electric field is large compared to the molecular rotational energy, rotation is suppressed in favor of libration about the direction of the electric field. The potential energy of the low-lying rotational levels then approaches $\mathcal{E} = -d_e E$ and is always negative [19]. In a spatially varying electric field, the resulting force is $\mathbf{F} = d_e \nabla E$ that, as for ground state atoms, is in the direction of increasing electric-field magnitude (strong field seeking).

As an example, consider cesium fluoride, which has a very large dipole moment [20] of $d_e = 2.65 \times 10^{-29}$ J/(V/m) [or 7.88 Debye, where 1 Debye = 3.36×10^{-30} J/(V/m)] and a small rotational constant [21] of $B_e = 0.27$ K (or 0.188 cm⁻¹). In its lowest angular momentum state ($J=0$), and traveling from a region of no field

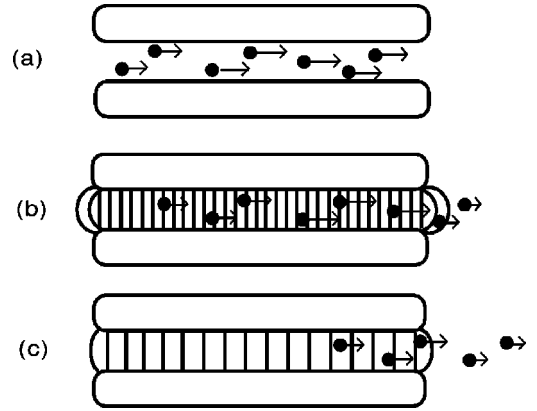


FIG. 2. Schematic diagram of longitudinal cooling with a time-varying electric-field gradient. The relative velocity of the particles is indicated by the length of their arrows and the electric-field strength by the density of field lines. A pulse of molecules or neutral atoms expands as it enters the plates with the fastest molecules or atoms in the lead (a). The same procedure as in Fig. 1 is followed except that the electric field decreases over time. The fastest, exiting first, lose more kinetic energy (b) than slower ones that exit later when the field gradient is smaller (c). Alternatively, if the field is turned on before all of the atoms have entered the electric-field plates, the slowest atoms are accelerated as they enter the plates. With sufficient field strength, the relative velocities of the slow and fast molecules can be interchanged and the pulse will rebunch.

to a region of 10^7 V/m, CsF gains kinetic energy, E_{kin} , by roughly the amount $\Delta E_{\text{kin}} = -\Delta\mathcal{E} = d_e(E_f - E_i) = 2.65 \times 10^{-22}$ J = 19 K. A more accurate value, calculated using the formulas from Von Meyenn [19], is 16 K. This is about 640 times larger than for Cs, as discussed earlier.

As in the atomic case, the final velocity of the CsF molecule, after traversing the potential, is $v_f^2 = 2(\Delta E_{\text{kin}})/M + v_i^2$, where v_i and v_f are the initial and final velocities, respectively, and M is the mass. For $v_i=0$, the final velocity for the example given above would be 45.7 m/s. Equivalently, a 45.7-m/s CsF molecule traveling from a region of 10^7 V/m electric field to a region of no field would be slowed to rest.

C. Slowing molecules and atoms

A practical apparatus for slowing should have the electric-field gradient perpendicular to the field. Otherwise, a beam of molecules or atoms traversing the electric-field gradient is likely to strike one of the surfaces used to form the electric field. A simple apparatus that meets this requirement is a set of parallel electric field plates (Fig. 1) attached to a voltage source that can quickly be ramped from zero.

To operate a set of electric-field plates as a time-varying electric-field-gradient slowing apparatus, we do the following. A neutral atom in its ground state enters the region between the electric-field plates with no field (the term atom also applies to clusters and molecules in strong field seeking states). With the atom between the electric-field plates, the voltage is turned on producing a uniform electric field. The potential energy of the atom is lowered by the electric field, but a spatially uniform, time-varying electric field does no work on a dipole, so there is no change in the kinetic energy of the atom. As the atom exits the plates passing through an

electric-field gradient to a zero-field region outside, it gains potential energy and loses kinetic energy. To accelerate an atom, the field is turned on before the atom enters the electric-field plates and is then turned off before the atom exits. The latter arrangement can also be used to slow a weak-field-seeking molecule.

The slowing process may be repeated by arranging a series of electric-field plates, each having a voltage applied once the atom has entered the uniform electric-field region. The energy change of the atom, traversing the sequence, is then cumulative. If a sufficient number of electric-field plate sections are assembled, it should be possible to slow a thermal beam of atoms to near rest.

This slowing process is analogous to but the reverse of the acceleration of charged particles in linear accelerators [22] and cyclic accelerators [23], where charged particles accelerate through a sequence of small voltage gradients. After each voltage gradient, the charged particles drift through a time-varying, but spatially uniform voltage, in which the voltage changes or reverses. This establishes a new voltage gradient without requiring successively higher voltages.

The same slowing principle can also be applied using large magnetic-field gradients on atoms or paramagnetic molecules. However, it is more difficult to switch strong magnetic fields.

D. Cooling and bunching

A decrease in the longitudinal velocity spread of the beam can be achieved by applying an electric field that decreases in time to atoms that have been arranged according to their velocity (Fig. 2). The first atoms exiting the plates are slowed more than the atoms exiting at later times when the electric field, and hence the electric-field gradient, have decreased. A beam of atoms will be ordered by velocity when a short pulse is allowed to spread.

This is a form of cooling even though the initial and final velocity distributions might not be Maxwell-Boltzmann. The process conserves phase space (the area enclosed in a plot of the relative velocity of each particle versus its relative position) and is analogous to the debunching of a charged particle beam in an accelerator. The process can also be reversed and used to bunch a beam so that more atoms arrive at a selected point at the same time. Bunching can reproduce or even compress the original longitudinal spatial distribution of a pulse of atoms—a useful technique for detecting weak signals.

III. EXPERIMENTAL RESULTS

A. Experimental arrangement

To test the principle of slowing and cooling with time-varying electric-field gradients, we slowed, cooled, and bunched packets of Cs atoms initially traveling 2 m/s using a single set of electric-field plates with fields of up to 5×10^6 V/m. The low initial velocity and large polarizability of Cs made it easy to observe and measure the slowing (0.20 m/s at 5×10^6 V/m), cooling, and bunching effects with a single electric-field region. A schematic of the apparatus is shown in Fig. 3.

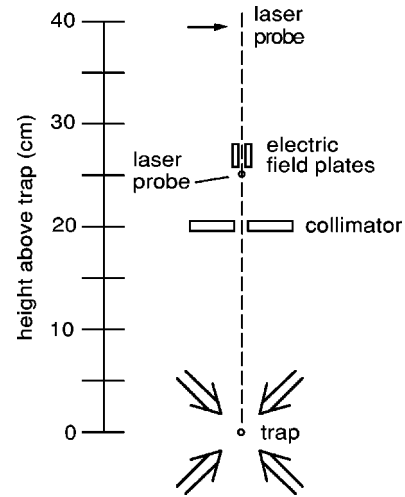


FIG. 3. Schematic of the apparatus used to test slowing and cooling. The vertical dimension, the collimator, and plate spacing, are to scale. The laser-probe beam below the electric-field plates is parallel to the plate gap and the probe above the plates is perpendicular to it. Only four of the six trapping lasers are shown.

Packets of Cs atoms were launched at rates of 0.25 Hz to 0.33 Hz from a vapor-capture magneto-optic trap constructed along the lines described in Refs. [24,25]. The laser beams that formed the x - y plane of the trap were oriented at 45 degrees to the vertical. This made it easier to perform measurements on the atoms after they had been launched. The trap temperature, determined by observing the expansion of the Cs cloud, was about 30 μ K. The trap laser system, which was stable and reliable, used an external cavity-grating configuration with piezo-electric tuning [26] and a Spectra Diode Labs model 5410-C diode laser with an anti-reflection coating on the front facet. To launch the Cs atoms, a pair of acousto-optic modulators blue (red) shifted the upward (downward) pointing laser beams by 5 MHz to form a moving molasses [25,27].

The tower into which the atoms were launched extends 55 cm above the trapping region. At 20 cm above the trap, a 1.3-cm aperture restricts the horizontal dimensions of the packet. At 27 cm above the trap, a pair of stainless-steel electric-field plates, each 2.2 cm tall by 1.7 cm wide, straddles the center line. Each electric-field plate is supported by a rod extending through a high-voltage vacuum feed through mounted on a bellows. The bellows allowed us to vary the spacing between the plates. Large-gap spacings of 6 mm and 8 mm were chosen to allow the maximum number of atoms through the plates, and to minimize defocusing effects at the edges of the plates. See Sec. III D for a discussion of the defocusing effects.

Two high-voltage-pulsed power supplies, one positive and one negative, were used to charge the electric-field plates. The heart of each power supply is an automobile ignition coil driven by a low current dc power supply that charges a capacitor in series with the input of the ignition coil [28]. Discharging the capacitor supplies the input pulse to the coil. For cooling and bunching experiments, a decaying voltage was produced by an RC circuit at the ignition coil output. The components of this RC circuit are the high-voltage coaxial cable (about 100 pF/m) from the ignition coil output to the high-voltage feed through, and a resistor to

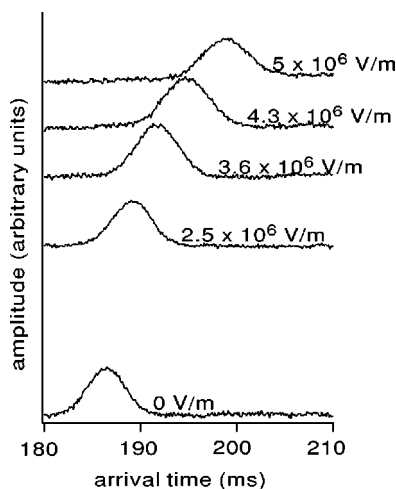


FIG. 4. Slowing of Cs atoms by time-varying electric-field gradients. The time of arrival at the upper probe is plotted for different electric fields used for the slowing. The horizontal scale is the time elapsed from when the magnetic field coils turn off for the launch. The vertical scale is the electric field and superimposed on each field setting is the inverted absorption signal at the upper probe.

ground. For slowing measurements, a high resistance was chosen to make the time constant long compared to the transit time of the atoms through the electric-field plates.

For Cs-atom time-of-flight velocity measurements, we formed probe-laser beams using a small fraction of the light from the trapping laser. One probe beam passed 0.5 cm below the electric-field plates and a second probe beam, perpendicular to the electric field, passed 14 cm above the first. The probe-beam intensities were measured with photodiodes. The signal for the atoms passing through a probe beam was the attenuation of the probe beam due to scattering by the passing atoms.

The launched atoms arrived at the electric-field plates in a packet 1.5 cm long—longer than the uniform region of the electric-field plates. It was easier to understand the results of slowing measurements if the packet of Cs atoms fit entirely within the uniform region. The packet was trimmed using the lower probe beam that deflected the atoms sufficiently so that they were not detected by the second probe. To accept only the center of the packet, the laser was shifted out of resonance for a few milliseconds. We were thus able to reduce the vertical size of the packet at the lower probe from 1.5 cm to about 0.3 cm. The arrival time of the atoms at the upper probe was measured relative to the launch time. The stability of the launch was checked by periodically measuring the arrival time at the lower probe.

B. Slowing

The time of arrival of the packet at the upper probe, as a function of the applied electric field, is shown in Fig. 4. The electric field was turned on after the Cs atoms entered the uniform-field region of the plates, and was kept nearly constant as the atoms exited the plates. Increasing the electric field delayed the arrival of the Cs atoms at the upper probe. The width of the packet increased because the packet had more time to spread.

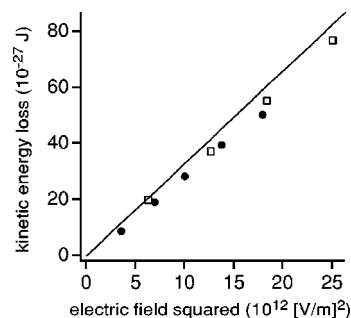


FIG. 5. Comparison of measured and calculated energy loss of Cs atoms traversing a time-varying electric-field gradient. The measurements were made with 6-mm (shown as open squares) and 8-mm (filled circles) plate spacings. The statistical uncertainties are within the size of each point. The expected energy loss, calculated from Eq. (2), is shown as a line. The systematic uncertainties are 2 percent for the Cs dipole polarizability and about 10 percent for our electric field. The observed differences between the measured and expected energy loss are within these uncertainties.

For a quantitative measurement of the slowing, we calculated the loss in kinetic energy, based on the increase in transit time, and plotted this quantity as a function of the square of the electric field. This is shown in Fig. 5. Two plate spacings, 6 mm and 8 mm, were used. We compare these data points with the expected energy loss, calculated from $\alpha E^2/2$ for $\alpha = 6.63 \times 10^{-39}$ J/(V/m)² [16]. The effect is clearly quadratic in the electric field and is close to the predicted size. The systematic error is consistent with the large uncertainty in our measurement of the electric field.

C. Cooling and compression

To cool and bunch the Cs atoms we matched the decay time of the electric field with the transit time of the atoms through the electric-field gradient. In addition, we used the full vertical size of the packet that at the plates was 1.5 cm and, without cooling or bunching, was 2.5 cm at the upper probe. With this short decay time, we were able to utilize two methods to cool and bunch the packets. In the first, the electric field was turned on once the whole packet had entered the uniform region. Here, the faster atoms exiting first were slowed more than the slower atoms, reducing the velocity spread. In the second method, we turned on the electric field once the faster atoms in the leading edge of the packet had entered the uniform region of the field, but while the slower atoms were still in the electric-field gradient. The slower atoms were accelerated into the plates while the fastest atoms, already in the uniform-field region, were unaffected. On exiting the plates, the field had decayed sufficiently so as not to affect the distribution. However, with plates of the proper length, additional cooling could be achieved on exit using the first method. Bunching occurs as the packet evolves if during the process the (initially) slow atoms are accelerated to a velocity greater than that of the fast atoms.

As an example, Fig. 6 shows the arrival time of the Cs atoms at the upper probe as a function of the electric field. The electric field is turned on when roughly half of the packet reaches the uniform-field region. The rest of the

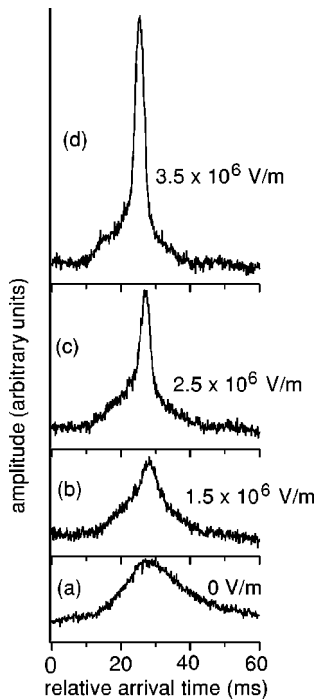


FIG. 6. Cooling and bunching of Cs atoms by time-varying electric-field gradients. The signal from the upper probe is shown as a function of the initial applied electric field, which has a decay time of 5 ms. The narrowing of the base in (b)–(d) is due to cooling of the atoms. The narrow peak, especially in (c) and (d) is due to the bunching of the atoms.

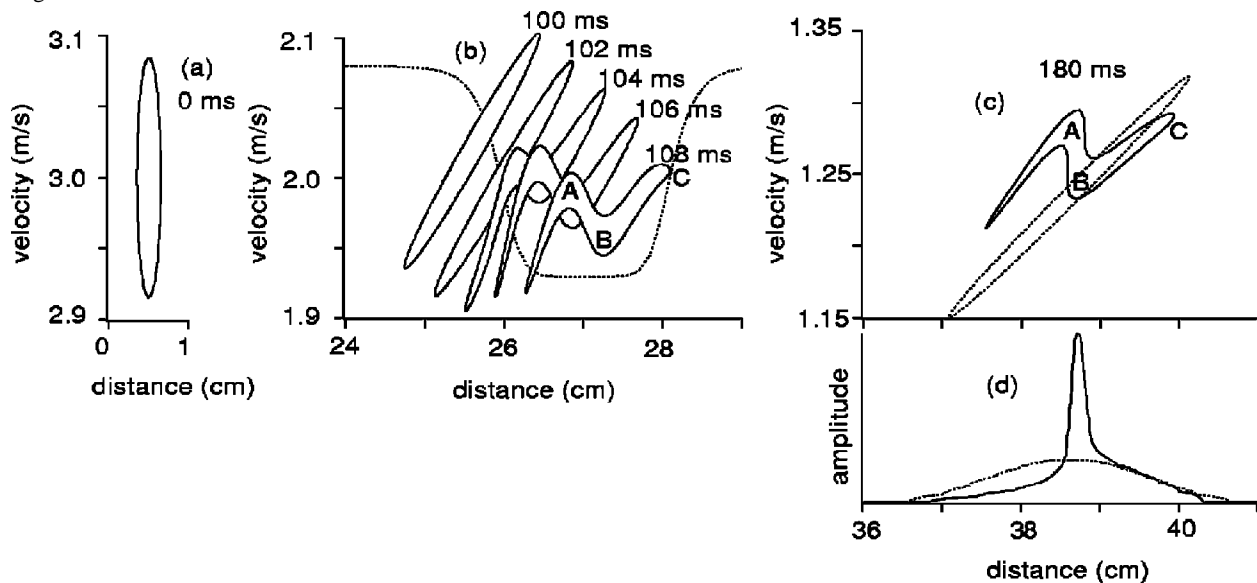


FIG. 7. Longitudinal phase space of the Cs atoms cooled and bunched in a time-varying electric-field gradient. The initial longitudinal phase space at launch, shown in (a), is approximated by an ellipse with a 3-mm spatial spread and a 0.15-m/s velocity spread. At 100 ms after launch, (b), the packet has spread to 1 cm and the velocity has decreased due to gravity. The electric field, which has a decay constant of 5 ms, is turned on at 103 ms as the slower atoms reach the electric-field gradient at the entrance of the plates. The dashed curve in (b) is the potential energy of the atoms due to the electric field. From 103–106 ms the slow atoms are accelerated while the faster atoms within the uniform field are unaffected. By 108 ms, the packet is past the electric-field gradient at the plate entrance and the electric field has decayed, so there is little force on the atoms as they exit the plates. In (b), the kink in the packet (marked A) is now at the same velocity as that of the right-most portion (marked C). The velocity spread of the packet has been nearly halved. As the packet time evolves, (c), the spatial separation between A and B does not change. In addition, the lowest velocity portion (marked B) is retarded and, at 180 ms, lies at the same spatial coordinate as A. When this occurs, we get a large peak in the absorption signal because the portion between A and B arrives at the probe, as a bunch, only a few millimeters wide (instead of the 2.5 cm for the uncompressed packet). The resulting calculated density profile of the packet is shown in (d). The dashed curves in (c) and (d) are the phase space and density profile, respectively, if no cooling has been utilized. The densities in (d) incorporate an initial assumed Gaussian phase-space distribution.

packet is still in the electric-field gradient. The electric field decays with a RC time constant of 5 ms, and the packet velocity at this point is roughly 2 m/s. The effects of cooling and then compression in Fig. 6 are striking. The transit time of the atoms through the upper probe is reduced from about 16 ms [full width at half maximum (FWHM)] at zero field, to 3 ms at 3.5×10^6 V/m. With a packet velocity of 1.2 m/s at the upper probe, the transit time corresponds to a packet length of about 3.6 mm, reduced from the original 1.5 cm at the electric-field plates (2.5 cm at the upper probe).

To compare the experimental results with the calculation, we modeled the time evolution of the longitudinal phase space of the Cs atoms for the experimental conditions in Fig. 6. The results are shown in Fig. 7. The electric field along the center line between the plates used to determine the potential energy of the Cs atoms at each point was calculated by a two-dimensional finite-element analysis program. The resulting potential energy is shown, superimposed on phase-space diagrams in Fig. 7(b).

In Fig. 8 we compare the observed Cs beam profile with the calculation in Fig. 7. The calculation, which is done in one dimension, assumes that the initial spatial distribution of atoms is Gaussian. The calculated spatial distribution has been converted into time, translated by about 5 ms, and scaled to align it to the data. There is good agreement between experiment and calculation, except for a small difference between the width of the calculated and observed peaks (possibly due to the simple assumptions used in the calculation).

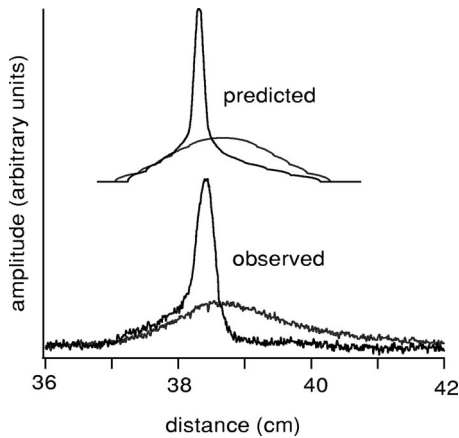


FIG. 8. Comparison of observed and predicted probe signals for the cooling and bunching of Cs atoms. The broad curves are for zero electric field and the peaks are for an initial electric field of 3.5×10^6 V/m that decays with a 5-ms time constant.

tion). We conclude that one can make reliable calculations of the effects of time-varying electric-field gradients on the phase-space evolution of atoms.

D. Defocusing

So far we have only discussed electric-field configurations in one dimension. For atoms on the midplane between two parallel plates there are no additional forces. However, for atoms in the fringe field of the plates and not on the midplane, there is a force toward the nearest plate. The magnitude of this force, which transversely defocuses the packet, depends on the shape of the edges of the electric-field plates. In general, any convex (concave) surface on a field plate produces a local increase in the electric-field gradient towards (away from) the surface. It should be stressed that the change in kinetic energy of the atoms is determined by the conservation of energy. All atoms will have their kinetic energy reduced by the same amount after exiting the electric field, even though some may have slightly changed direction.

The defocusing effects can be minimized by using an electric-field plate gap that is large compared to the width of the beam of atoms. However, increasing the gap increases the voltage needed to produce the same electric field and reduces the maximum electric field that can be sustained. For simplicity in this experiment, we chose a small gap-to-beam-width ratio and tolerate some defocusing. However, there are more elaborate field configurations for which our calculations show very small defocusing effects. In Fig. 9, we compare one such set of electric-field plates with field plates having a simple parallel-plate geometry. For an atom slightly off the midplane, the transverse force is reduced by about a factor of 6 compared to the simple plate geometry. We will discuss details of focusing and defocusing in a future paper.

IV. APPLICATIONS

A. Slowing thermal beams of atoms and molecules

1. Electric fields

While electric fields of 10^7 V/m or higher can be maintained by ordinary metal electrodes with a small gap spacing,

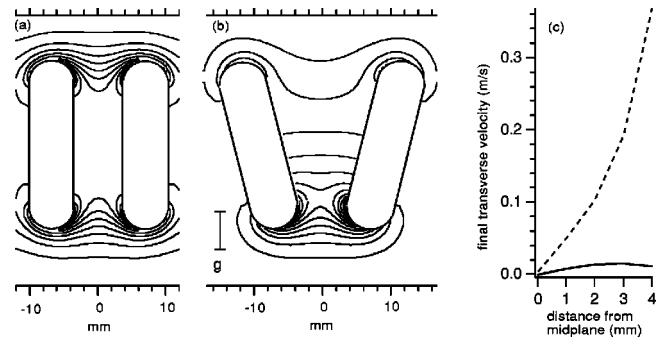


FIG. 9. Defocusing effects for simple parallel- and splayed-electric-field plates. In (a) and (b) the schematics of the two electric-field plate configurations are shown to the same scale, along with the lines of constant energy potential [$\mathcal{E} = -(1/2)\alpha E^2$] for Cs from an applied voltage of 40 kV. For comparison the interval corresponding to the force of gravity labeled g , is shown in (b). In the parallel plate configuration (a) used for the measurements in this paper, the potential contours curve and atoms not on the midplane acquire transverse velocities as they exit. In (b), the field plates are splayed 15° from vertical producing a potential minimum just above the bottom of the plates. On (b) the voltage would be applied once the atom packet, traveling from below, has passed beyond the potential minimum. The contours further up are much flatter than in (a), and the defocusing is considerably less. The resulting transverse velocity for an initial longitudinal velocity of 2 m/s is shown in (c). The dashed line corresponds to the simple parallel plates in (a) and the solid line corresponds to the splayed plates in (b).

much stronger fields can be maintained by heated glass cathodes [29]. Glass cathode systems have been used to produce large Stark effects in beams of Cs [30] and Tl atoms [31]. A set of 75-cm-long all-glass electric-field plates have operated at 4.5×10^7 V/m [31]. Short electric-field plates with a heated glass cathode at ground potential and a metal anode have sustained electric fields of 5×10^7 V/m and higher [30].

2. Slowing ground-state atoms

Atoms that are of interest for slowing and cooling by time-varying electric-field gradients are those with large dipole polarizabilities that cannot be laser slowed and cooled. The dipole polarizabilities are largest in alkali metals and alkali earths. However, actinides, lanthanides, and transition elements near an alkali also have polarizabilities [17] above 1×10^{-39} J/(V/m)², compared to 6.63×10^{-39} J/(V/m)² for Cs, which has the highest known ground-state polarizability.

As an example, we consider slowing a thermal beam of neutral americium (atomic number 95) to near rest. With a polarizability [17] of 2.59×10^{-39} J/(V/m)², each 5×10^7 V/m slowing section will reduce the kinetic energy by 0.23 K. It is impractical to slow atoms from the peak of the velocity distribution at the 1500 K needed to form a beam of Am. However, if one is willing to sacrifice intensity, the slower atoms from the low-velocity tail of the thermal velocity distribution are available. The low-velocity atoms from thermal distributions are often used to load magneto-optic traps, either from a vapor inside the chamber [24] (as we have done) or from an atomic beam [32,33]. Recently, Ghaffari *et al.* [33] developed an atomic low-pass velocity filter that passes slow atoms and blocks fast atoms.

For the Am velocity distribution tail at 1 K (8.4 m/s), only about five time-varying electric-field-gradient slowing sections would be needed to bring the atoms to near rest. The maximum energy spread that can be accepted by a single section is about equal to the energy decrease in one section, which for Am is about 0.23 K. Based upon a Maxwell-Boltzmann velocity distribution inside a 1500-K effusive oven with a thin orifice [34], roughly 10^{-7} of the atoms in a beam will be in the energy range from 0.89 K to 1.1 K. (About 4×10^{-7} of the atoms in a beam will be within the energy range 3.60 K to 3.83 K.)

The final velocity and the minimum length of the electric-field plates will determine the repetition rate for slowing packets of atoms. At the last field plate section where the distance between pulses will be at a minimum, one pulse of atoms must exit before the next pulse enters. The total number of atoms that reach the end of the apparatus thus depends on the final velocity, the length of the apparatus, the initial velocity, and on any focusing available.

A method for focusing strong-field-seeking atoms and molecules using alternating electric-field gradients [35] has been applied to molecular beams [36]. The range of beam energies that can be accepted can also be increased by using a design that cools over several electric-field sections before slowing. We will discuss some of these details in a future paper.

For clusters [15,37], the polarizability per atom of small homonuclear alkali clusters is close to the atomic polarizability, and decreases to a value of about 0.4 times the polarizability per atom for bulk samples [38]. It should be possible to slow and cool clusters in the same way as atoms.

We also note that the metastable states of noble gases have dipole polarizabilities [14] that are of the order of $10 \times 10^{-39} \text{ J/(V/m)}^2$. This would allow noble-gas atoms in the metastable states to be slowed and cooled, much the same way as ground-state (Cs) atoms. They do, however, have large tensor polarizabilities, which may permit effective slowing and cooling of only a single angular momentum state.

3. Slowing Rydberg atoms

The properties of Rydberg atoms [39], atoms in states of very high principle quantum number n , are similar for all elements and include very large dipole polarizabilities [14] that can be either positive or negative. This makes Rydberg states worth considering for slowing atoms. Slowing of Rydberg atoms in inhomogeneous electric fields was proposed by Breeden and Metcalf [40], who analyzed the case of time-independent inhomogeneous electric fields, and atoms in short-lived Rydberg levels.

To slow Rydberg atoms using time-varying electric-field gradients, a number of conditions must be met. The lifetimes of the states must be long enough to pass through the apparatus and the electric field must neither quench the state nor ionize the atom, but should still be large enough to produce significant slowing. The lifetime of a state in a quasihydrogenic Rydberg atom with principle quantum number n and angular momentum l has been calculated by Chang [41] who finds for high angular momentum, $\tau = 93n^3(l+0.5)^2$, where τ is the lifetime in ps. For $n=30$, the lifetimes are about 2.2 ms for $l=29$ and about 1.1 ms for $l=20$. An external electric

field mixes different values of l having the same z component of angular momentum m . Thus, only the sublevels with large values of m will have unquenched lifetimes, since the lower m states mix with low l states that have much shorter lifetimes.

The critical electric field for ionizing a Rydberg atom is given classically as $E_{cr} = 1/(16n^4)$, where E_{cr} is in atomic units (of $5.14 \times 10^{11} \text{ V/m}$ [42]). High m states are more circular and thus require a higher field to ionize. The Stark effect also modifies the critical field [39] and for blue shifted levels the critical field may be closer to $1/(12n^4)$.

The change in energy levels with the electric field has been calculated by Bethe and Salpeter [43]. For a hydrogenic case they find in atomic units ($1 \text{ a.u.} = 1.0973 \times 10^7 \text{ m}^{-1}$), $W = -0.5n^2 + 1.5En(n_1 - n_2) - E^2n^4[17n^2 - 3(n_1 - n_2)^2 - 9m^2 + 19]/16$, where n_1 and n_2 are parabolic quantum numbers that satisfy the equation $n = n_1 + n_2 + |m| + 1$. Setting E equal to $1/(12n^4)$, we find that for $n=30$ and $l=20$ the energy change at the maximum field that does not ionize the atom is about 5.6 K or 7.6 K, depending on whether the red or blue shifted level is chosen. For the circular state, $|m|=n-1$ and $n_1=n_2=0$, the electric field cannot mix states from the same n or lower n , and the shift is much smaller. For $n=30$ and $l=29$, the maximum energy change before ionization is about 0.66 K.

4. Slowing polar molecules

Time-varying electric-field-gradient slowing and cooling of polar molecules with large electric dipole moments can be very efficient. As examples, we consider two linear diatomic molecules with large dipole moments: cesium fluoride, which has a small rotational constant, and lithium hydride, which has a very large rotational constant.

As discussed in Sec. II, a rigid rotor model calculation [19] of CsF in its lowest rotational state ($J=m=0$) shows that CsF would lose about 16 K of energy exiting each 10^7 -V/m electric-field section. The next few higher rotational levels [Fig. 10(a)] would also experience large changes in kinetic energy and could be efficiently slowed and cooled. With a 5×10^7 -V/m electric field, the change in kinetic energy [see Fig. 10(a)] for the lowest rotational level would be about 89 K, or equivalently a molecule traveling 98 m/s could be brought to rest. Longitudinal cooling of about 89 K could also be achieved in a single time-varying electric-field-gradient section.

In a thermal beam of CsF formed [44] at 850 K, about one-half percent of the molecules have a kinetic energy of 89 K or less. A disadvantage of using a thermal beam of molecules with a small rotational constant is that only a very small fraction of the molecules are found in any single rotational state. Only about one in 15000 CsF molecules are found in the $J=m=0$ state in a thermal molecular beam at this temperature [44].

An alternative approach is to form a supersonic beam [45] of CsF. The supersonic beam has a much lower internal temperature, which greatly increases the population of low rotational levels, and it is a very directional beam with a narrow velocity distribution. However, the beam velocity of a supersonic source is higher than the most probable velocity from an effusive source of the same temperature and has no low velocity tail. Slowing a supersonic CsF beam would re-

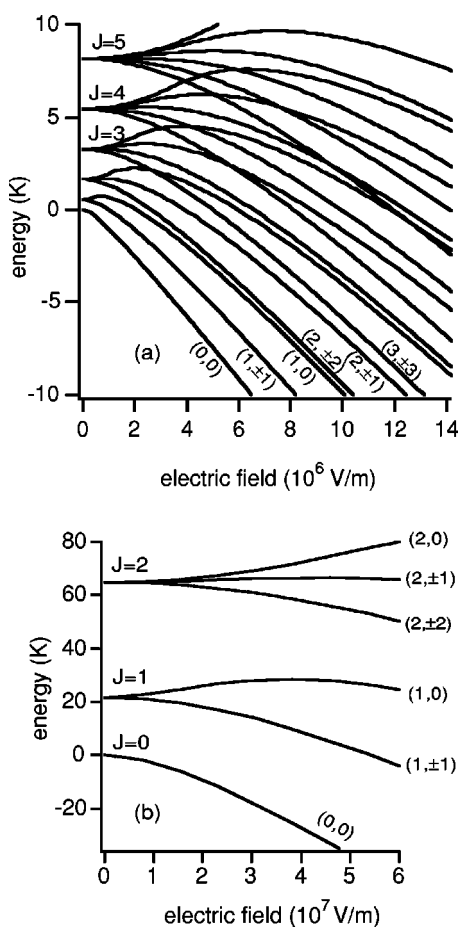


FIG. 10. Energy levels of the low rotation levels of CsF (a) and LiH (b) in electric fields. The calculation is based on the equations in von Meyenn [19] who uses a rigid rotor model. The energy is in units of kelvins ($1 \text{ K} = 0.69 \text{ cm}^{-1}$). Note the different scales for the electric field in (a) and (b).

quire approximately twenty electric-field sections—still very doable.

Lithium hydride and other metal hydrides have both very large rotational constants and large dipole moments. For LiH, $B_e = 11 \text{ K}$ (7.5 cm^{-1}) and $d_e = 2.0 \times 10^{-29} \text{ J/(V/m)}$ (5.9 Debye) [21,20]. Even at $5 \times 10^7 \text{ V/m}$, the electric field does not completely suppress rotation [Fig. 10(b)], and for the $m=0$, $J \neq 0$ states, the interaction energy is both large and positive. As shown in Fig. 10(b), a LiH molecule in the $J=1$, $m=0$ state entering an electric field of $3.5 \times 10^7 \text{ V/m}$ would lose about 7 K of energy. And since the rotation constant is large, a significant fraction of the molecules in a thermal beam are in low rotation states. Approximately 2×10^{-5} of the LiH molecules in a beam from a 1200-K effusive oven will have an energy of 7 K or less. Those in the $J=1$, $m=0$ state could be slowed to rest with a single electric-field section.

Lithium hydride in the low-lying $m=0$, $J \neq 0$ states and other molecular states that have positive interaction energies are weak-field seeking and can be transversely focused by static multipole electric fields [46]. (For focusing strong-field-seeking states see Refs. [35,36].) It may also be possible to trap weak-field-seeking states in electric field traps [7–10,12] or a laser trap [11]. An electric-field trap could, in principle, be up to 7.5-K deep for the $J=1$, $m=0$ state of

LiH, depending on the electric field that can be sustained in the trap geometry.

The $J=1$, $m=0$ and $J=2$, $m=0$ rotational levels of CsF have negative interaction energies at strong electric fields, but positive interaction energies at weaker fields [Fig. 10(a)]. Thus, CsF in these states could be efficiently slowed using strong electric-field gradients, then focused and trapped in a weaker electric field. The change in kinetic energy exiting a $5 \times 10^7 \text{ V/m}$ electric field would be 82 K (74 K) for the $J=1$, $m=0$ ($J=2$, $m=0$) state, while in an electric field of $2.5 \times 10^6 \text{ V/m}$ ($4 \times 10^6 \text{ V/m}$) the $J=1$, $m=0$ ($J=2$, $m=0$) state would be weak-field seeking with an interaction energy of 0.5 K (1 K). Alternatively, CsF could be slowed in the $J=1$, $m=1$ state and then in a weak electric field transferred to the $J=1$, $m=0$ state by an rf transition [44].

B. Application to cold atoms

1. Measurement of the ground-state dipole polarizability of atoms

Figure 5 demonstrates the sensitivity of time-varying electric-field-gradient slowing to the static dipole polarizability. Each data point in this figure represents less than 300 seconds of counting. Key quantities in a time-varying electric-field-gradient measurement of dipole polarizabilities are the electric-field strength, the beam velocities, and the electric-field profile at the plate exit and/or entrance. The field profile is needed to determine the drift lengths before and after slowing for a time-of-flight velocity measurement. We expect that with a moderate effort, polarizability measurements on alkali, alkaline earth, and other slow, cold atoms can be made to an accuracy of a few parts per thousand [47].

Although dipole polarizability is related to many important physical and chemical properties [17], the ground-state dipole polarizability has been measured in fewer than 20 percent of the known elements [17]. And of these, only for the noble gases and sodium [48] has an accuracy of one percent been surpassed [17]. The traditional method for measuring the static dipole polarizabilities of condensable atoms is the elegant electric-magnetic-field-gradient balance technique (E - H balance) [14,49], which uses thermal beams of atoms. Slow, cold atoms would also allow a significantly improved accuracy for E - H balance and other deflection-based methods. However, we anticipate that time-varying electric-field-gradient slowing (or acceleration) will be easier to perform and poses fewer challenges to understanding the distributions of electric field and atoms.

2. Beam transport

Inhomogeneous magnetic fields are used for transverse focusing of laser-cooled atom packets [50], and Cornell, Monroe, and Wieman [51] have used time-varying inhomogeneous magnetic fields to radially and axially focus atoms being transferred between traps. Time-varying electric-field gradients are a useful complement to these atom-optic elements because they are insensitive to the magnetic or hyperfine substates, and when edge effects are small or absent, they control only in the longitudinal direction.

One possible application of the time-varying electric-field gradient to beam transport is to longitudinally spread atoms

in a cold Cs atom atomic clock, to reduce collisional frequency shifts [52]. In such a clock, the atoms would be spread before they passed through the first rf region (or the first passage through the single rf region in a fountain clock) and, if necessary, to sharpen the detection signal rebunched after they passed through the second rf region (after their return through the rf region in a fountain clock). The magnetic fields associated with turning on and off the electric field can be made small so as not to influence the magnetic shielding environment of the clock.

3. Launching atoms

If a set of electric-field plates is turned on near a cloud of cold confined atoms in the ground state, the atoms will accelerate into the plates. Turning off the field when the atoms are in the uniform-field region then allows the atoms to exit the plates with a net velocity. Cesium atoms entering an electric field of 4×10^7 V/m will accelerate from rest to 6.8 m/s.

The electric-field plates can be positioned to launch atoms in any direction. To launch horizontally, a vertical gap will provide a fringe field at the bottom that can help keep the atoms from falling out of the plates. To launch vertically, the electric-field gradient at the initial location of the atoms needs to be large enough to overcome gravity. In microgravity, the initial acceleration needs only to be large enough that the cloud of atoms does not expand beyond the dimensions of the electric-field plate gap (to prevent the loss of atoms). It would also be easy to vary the launch velocity and direction.

One possible arrangement of electric-field plates is to invert the plate configuration shown in Fig. 9(b).

Note added in proof. Recently, Bethlem, Berden, and Meijer [Phys. rev. Lett. **83**, 1588 (1999)] have reported using a 63-stage time-varying electric-field-gradient apparatus to slow metastable CO molecules from 225 to 98 m/s. Also Gupta and Herschbach (<http://itamp.harvard.edu/trappingabstracts.html#anchor61968>) have reported slowing Kr and Xe using a supersonic molecular beam source nozzle mounted on the periphery of a rotor spinning fast enough to offset the flow velocity from the source.

ACKNOWLEDGMENTS

We are grateful to Douglas McColm for many stimulating and fruitful discussions and for his help in clarifying several key concepts. We thank Timothy Page, Andrew Ulmer, Christopher Norris, Karen Street, and Otto Bischof for assistance in constructing the apparatus, and thank C.C. Lo for developing a very functional and cost-effective time-varying high-voltage power supply. One of us (J.M.) thanks the Environment, Health, and Safety Division at LBNL, and especially Rick Donahue and Roberto Morelli, for help with computing resources, and one of us (H.G.) thanks Alan Ramsey for timely inspiration. This work was supported by the Office of Science, Office of Basic Energy Sciences, of the U.S. Department of Energy under Contract No. DE-AC03-76SF00098. One of us (J.M.) is partially supported by the National Science Foundation.

-
- [1] J. M. Doyle, B. Friedrich, J. Kim, and D. Patterson, Phys. Rev. A **52**, R2515 (1995).
- [2] H. von Busch, W. Demtröder, Vas Dev, H.-A. Eckel, R. Großkloß, M. Keil, H.-G. Krämer, T. Platz, and H. Wenz, Phys. Scr. **T78**, 24 (1998); R. E. Miller, in *Atomic and Molecular Beam Methods*, edited by G. Scoles (Oxford University Press, New York, 1992), Vol. 2, p. 196.
- [3] R. N. Zare, Science **279**, 1875 (1998); (private communication).
- [4] See, for example, U. Valbusa, in *Atomic and Molecular Beam Methods* (Ref. [2]), Vol. 2, p. 327; G. Boato, *ibid.*, Vol. 2, p. 340.
- [5] See, for example, L. Mattera, in *Atomic and Molecular Beam Methods* (Ref. [2]), Vol. 2, pp. 366; R. B. Doak, *ibid.*, Vol. 2, p. 384; D. J. Auerbach, *ibid.*, Vol. 2, p. 444; G. Comsa and B. Poelsma, *ibid.*, Vol. 2, p. 463; M. Asscher and G. A. Somorjai, *ibid.*, Vol. 2, p. 488.
- [6] For a discussion on trapping molecules, see, for example, D. Herschbach, Rev. Mod. Phys. **71**, S411 (1999).
- [7] D. P. Katz, J. Chem. Phys. **107**, 8491 (1997).
- [8] W. H. Wing, Phys. Rev. Lett. **45**, 631 (1980).
- [9] T. Takekoshi, J. R. Yeh, and R. J. Knize, Opt. Commun. **114**, 421 (1995).
- [10] S. K. Sekatskii, Pis'ma Zh. Éksp. Teor. Fiz. **62**, 900 (1995) [JETP Lett. **62**, 916 (1995)]; S. K. Sekatskii and J. Schmiedmayer, Europhys. Lett. **36**, 407 (1996); see also J. Denschlag, G. Umshaus, and J. Schmiedmayer, Phys. Rev. Lett. **81**, 737 (1998).
- [11] B. Friedrich and D. Herschbach, Phys. Rev. Lett. **74**, 4623 (1995).
- [12] T. Seideman, J. Chem. Phys. **106**, 2881 (1997); **107**, 10 420 (1997).
- [13] J. D. Weinstein, R. deCarvalho, T. Guillet, B. Friedrich, and J. M. Doyle, Nature (London) **395**, 148 (1998); J. D. Weinstein, R. deCarvalho, and J. M. Doyle, J. Chem. Phys. **110**, 2376 (1999); J. D. Weinstein, R. deCarvalho, K. Amar, A. Boca, B. C. Odom, B. Friedrich, and J. M. Doyle, *ibid.* **109**, 2656 (1998).
- [14] See, for example, T. M. Miller and B. Bederson, in *Advances in Atomic and Molecular Physics*, edited by D. R. Bates and B. Bederson (Academic Press, New York, 1977), Vol. 13, p. 1.
- [15] See, for example, K. D. Bonin and M. A. Kadar-Kallen, Int. J. Mod. Phys. B **8**, 3313 (1994).
- [16] R. W. Molof, H. L. Schwartz, T. M. Miller, and B. Bederson, Phys. Rev. A **10**, 1131 (1974).
- [17] T. M. Miller, in *CRC Handbook of Chemistry and Physics*, 79th ed., edited by D. R. Lide (CRC Press, Boca Raton, FL, 1998), Chap. 10, p. 160.
- [18] See, for example, C. H. Townes and A. L. Schawlow, *Microwave Spectroscopy* (McGraw-Hill, New York, 1955), pp. 248–255; N. F. Ramsey, *Molecular Beams* (Oxford University Press, London, 1955), pp. 287–298.
- [19] K. von Meyenn, Z. Phys. **231**, 154 (1970).
- [20] D. R. Lide, in *CRC Handbook of Chemistry and Physics* (Ref. [17]), Chap. 9, p. 42.
- [21] Values taken from S. V. Khristenko, A. I. Maslov, and V. P.

- Shevelko, *Molecules and Their Spectroscopic Properties* (Springer, Berlin, 1998).
- [22] G. A. Ising, *Ark. Mat., Astron. Fys.* **18**, No. 30, 1 (1924); R. Wideröe, *Arch. Elektrotech.* (Berlin) **21**, 387 (1928).
- [23] E. O. Lawrence and N. E. Edlfsan, *Science* **72**, 376 (1930); E. O. Lawrence and M. S. Livingston, *Phys. Rev.* **37**, 1707 (1931).
- [24] C. Monroe, W. Swann, H. Robinson, and C. Wieman, *Phys. Rev. Lett.* **65**, 1571 (1990); K. Lindquist, M. Stephens, and C. Wieman, *Phys. Rev. A* **46**, 4082 (1992).
- [25] C. R. Monroe, Ph.D. Thesis, University of Colorado, 1992.
- [26] See, for example, R. W. Fox, L. Hollberg, and A. S. Zibrov, in *Experimental Methods in The Physical Sciences: Atomic, Molecular, and Optical Physics: Electromagnetic Radiation*, edited by F. B. Dunning and R. G. Hulet (Academic Press, San Diego, CA, 1997), p. 77.
- [27] M. Kasevich, E. Riis, S. Chu, and R. De Voe, *Phys. Rev. Lett.* **63**, 612 (1989); A. Clairon, C. Salomon, S. Guellati, and W. D. Phillips, *Europhys. Lett.* **16**, 165 (1991).
- [28] C. C. Lo (private communication).
- [29] J. J. Murray, Lawrence Radiation Laboratory Report No. UCRL-9506, 1960 (unpublished).
- [30] R. Marrus, E. C. Wang, and J. Yellin, *Phys. Rev.* **177**, 122 (1969).
- [31] H. Gould, *Phys. Rev. A* **14**, 922 (1976).
- [32] A. Cable, M. Prentiss, and N. P. Bigelow, *Opt. Lett.* **15**, 507 (1990); B. P. Anderson and M. A. Kasevich, *Phys. Rev. A* **50**, R3581 (1994).
- [33] B. Ghaffari, J. M. Gerton, W. I. McAlexander, K. E. Strecker, D. M. Homan, and R. G. Hulet, *Phys. Rev. A* **60**, 3899 (1999).
- [34] See, for example, H. Pauly, in *Atomic and Molecular Beam Methods*, edited by G. Scoles (Oxford University Press, New York, 1988), Vol. 1, p. 83.
- [35] D. Auerbach, E. E. A. Bromberg, and L. Wharton, *J. Chem. Phys.* **45**, 2160 (1966).
- [36] D. Kakati and D. C. Lainé, *Phys. Lett.* **24A**, 676 (1967); **28A**, 786 (1969); A. Lübbert, F. Günther, and K. Schügerl, *Chem. Phys. Lett.* **35**, 210 (1975).
- [37] K. D. Bonin and V. V. Kresin, *Electric-Dipole Polarizabilities of Atoms, Molecules and Clusters* (World Scientific, Singapore, 1997).
- [38] W. D. Knight, K. Clemenger, W. A. de Heer, and W. A. Saunders, *Phys. Rev. B* **31**, 2539 (1985).
- [39] See, for example, T. F. Gallagher, *Rydberg Atoms* (Cambridge, Cambridge, 1994), and references therein.
- [40] T. Breeden and H. Metcalf, *Phys. Rev. Lett.* **47**, 1726 (1981).
- [41] E. S. Chang, *Phys. Rev. A* **31**, 495 (1985).
- [42] T. W. Ducas, M. G. Littman, R. R. Freeman, and D. Klepner, *Phys. Rev. Lett.* **35**, 366 (1975).
- [43] H. Bethe and E. E. Salpeter, *Quantum Mechanics of One and Two Electron Atoms* (Springer, Berlin, 1957), p. 233.
- [44] H. K. Hughes, *Phys. Rev.* **72**, 614 (1947).
- [45] See, for example, M. D. Morse, in *Experimental Methods in The Physical Sciences: Atomic, Molecular, and Optical Physics: Electromagnetic Radiation*, edited by F. B. Dunning and R. G. Hulet (Academic Press, San Diego, CA, 1997) p. 21, and references therein; D. R. Miller, in *Atomic and Molecular Beam Methods* (Ref. [34]), Vol. 1, p. 14, and references therein. A very light carrier gas such as helium is often deliberately used to produce high-velocity supersonic beams. However, heavy carrier gases would produce lower velocity beams.
- [46] See, for example, V. A. Cho and R. B. Bernstein, *J. Phys. Chem.* **95**, 8129 (1991), and references therein.
- [47] An electric-field-gradient slowing measurement of the Cs dipole polarizability is currently underway in our laboratory.
- [48] C. R. Ekstrom, J. Schmiedmayer, M. S. Chapman, T. D. Hammond, and D. E. Pritchard, *Phys. Rev. A* **51**, 3883 (1995).
- [49] A. Salop, E. Pollack, and B. Bederson, *Phys. Rev.* **124**, 1431 (1961).
- [50] See, for example, W. G. Kaenders, F. Lison, I. Müller, A. Richter, R. Wyands, and D. Meschede, *Phys. Rev. A* **54**, 5067 (1996).
- [51] E. A. Cornell, C. Monroe, and C. E. Wieman, *Phys. Rev. Lett.* **67**, 2439 (1991).
- [52] E. Tiesinga, B. J. Verhaar, H. T. C. Stoff, and D. van Bragt, *Phys. Rev. A* **45**, R2671 (1992); K. Gibble and S. Chu, *Phys. Rev. Lett.* **70**, 1771 (1993).